

Structural Analysis of ZON-Type Aluminophosphates by Solid State NMR

A. Bailly,[†] J. P. Amoureux,[†] J. W. Wiench,[‡] and M. Pruski^{*,‡}[†]Université de Lille-1, F-59655 Villeneuve d'Ascq Cedex, France, and Ames Laboratory, Iowa State University, Ames, Iowa 50011

Received: August 2, 2000; In Final Form: October 16, 2000

Solid-state NMR spectroscopy has been used to study the new aluminophosphate material $\text{AlPO}_4\text{-ZON}$. Highly resolved multiple quantum magic-angle spinning NMR spectra showed all four Al sites in the framework of $\text{AlPO}_4\text{-ZON}$. Additional ^{27}Al resonances were detected in some samples. They were assigned to an impurity phase of $\text{AlPO}_4\text{-AFR}$ and to six-coordinated aluminum in the extra-lattice positions. High-speed MAS NMR of ^1H yielded the OH concentration in the samples synthesized from the fluoride-modified gels of different pH. The location of fluorine in the $\text{AlPO}_4\text{-ZON}$ framework has been verified by measuring the internuclear distances between ^{19}F and all ^{27}Al sites using the MQ-REDOR technique. MQ-REDOR has been also used to measure the distances between ^1H and ^{27}Al nuclei in this material.

1. Introduction

Zeolites, aluminophosphates, and other crystalline microporous molecular sieves are widely applied in the oil, petrochemical, and chemical industries, typically in catalysis and separation. Potential areas for their use depend on the pore structure and the charge distribution within the framework. Successful routes for hydrothermal synthesis of novel phases of these materials are sought via identification of the relevant synthetic parameters. Introduction of fluoride into the known synthetic recipes can modify the structure and the catalytic activity of microporous materials.¹ In 1996, Akporiaye et al.² reported the synthesis method of a fluorinated AlPO_4 aluminophosphate, called UiO-7, with a new structure of the ZON-type.³ More recently, Sierra et al.⁴ studied the influence of the synthesis parameters on the formation of $\text{AlPO}_4\text{-ZON}$ and related materials.

The UiO-7 aluminophosphates were synthesized between 120 and 180 °C from gels of the following composition: P_2O_5 ; Al_2O_3 ; [a] $(\text{CH}_3)_4\text{NCl}$ (tetramethylammonium chloride, TMACl); [b] HF; [c] $(\text{HOCH}_2\text{CH}_2)_2\text{NH}$ (diethanolamine, DEA) and $80\text{H}_2\text{O}$. In this synthesis, TMACl was used as a template and DEA served as a pH modifier. The ^{13}C magic angle spinning (MAS) NMR spectra of as-synthesized samples ruled out the presence of DEA.⁴ The only resonance detected by this method was located at 57.7 ppm, and was attributed to the TMA^+ ($(\text{CH}_3)_4\text{N}^+$) cations. It is noted that in the absence of F^- anions, which in UiO-7 compensate the TMA^+ cations, the above synthesis produced $\text{AlPO}_4\text{-20}$ with a sodalite-type structure.⁵ The high-resolution synchrotron X-ray powder diffraction (XRD) study of UiO-7 showed that its lattice is orthorhombic with $Pbca$ primitive space group and $a = 14.53 \text{ \AA}$, $b = 15.33 \text{ \AA}$, $c = 16.60 \text{ \AA}$, and $V = 3697 \text{ \AA}^3$.² Removal of the template (TMA^+) by calcination in air at 600 °C followed by dehydration deformed the lattice, such that $a = 14.47 \text{ \AA}$, $b = 14.84 \text{ \AA}$, $c = 17.48 \text{ \AA}$, $V = 3754 \text{ \AA}^3$.⁴ The extended framework of UiO-7

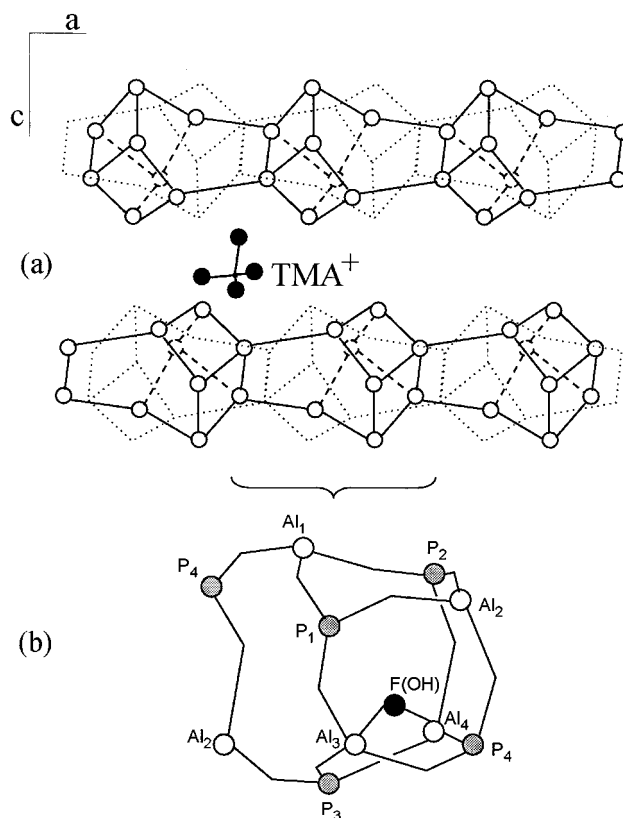


Figure 1. Structure of UiO-7 aluminophosphate. (a) [001] projection of the framework along the main 8-ring channel showing the alternative nature of the subunit chains and the position of the TMA^+ cations. (b) Detailed view of the structural subunit, with the aluminum atoms shown in white, phosphorus in gray and fluorine/OH site in black.

forms a two-dimensional channel system that is accessed through 8-ring windows. The framework is made up of cage-like units that are connected in $[4^4 6^2]$ chains parallel to the a axis (see Figure 1a). Adjacent chains are the translated mirror images of each other with respect to the ac plane. The TMA^+ cations fully occupy the 14-hedral $[4^6 6^4 8^4]$ cages formed at the intersection of the two 8-ring channels. Fluoride atoms are located in the

* Author to whom correspondence should be addressed at 230 Spedding Hall, Ames Laboratory, Iowa State University, Ames, IA 50011. E-mail: mpruski@iastate.edu.

[†] Université de Lille-1.

[‡] Iowa State University.

TABLE 1: Concentration of Fluorine in the Unit Cell $\text{Al}_{32}\text{P}_{32}\text{O}_{128}\text{TMAF}_x\text{TMAOH}_{8-x}$ (as determined in ref 4 by chemical shift analysis (x_{CA}) and in this work by NMR (x_{NMR}) versus the concentration of DEA [c]

sample	[c]	initial pH	final pH	x_{CA}	x_{NMR}
1	1.0	3.5	7.0	7.7	7.5 ± 0.2
2	1.5	4.5	8.5	4.9	6.0 ± 0.5
3	2.0	6.0	9.0	5.0	5.5 ± 0.5
4	3.0	7.5	10.0	4.5	4.5 ± 1.0

[4^{462}] cages between the pairs of Al atoms, giving them 5-fold coordination. Thus, fluoride bridges one of the 4-rings and points into the subunit, as shown in Figure 1b. The ^{19}F MAS NMR spectrum of UiO-7 (not shown) consists of a single line at -109 ppm (from CFCl_3), which indicates that F^- anions are located in a single type of environment. Figure 1b also shows four different phosphorus sites. In agreement with the XRD data, ^{31}P MAS NMR yielded three resonances at -16.5 , -20 , -32 ppm (with respect to 85% solution of H_3PO_4 in H_2O) with intensities 1:2:1.² They have been assigned to sites P_3 , P_1+P_4 , and P_2 , respectively, as explained in ref 2.

In this work, an NMR analysis of several UiO-7 compounds is presented. Multiple quantum magic angle spinning (MQMAS) NMR is used to identify the Al sites and to determine the structural purity of these materials. The location of fluorine in UiO-7 is of particular interest since, at present, the calcination process results in its removal from the lattice.² Since the XRD method is not effective in discriminating between the F^- atoms and the OH^- groups, a combination of MQMAS and rotational echo double resonance (MQ-REDOR)^{7,8} is used to establish the structure of these species.

2. Experimental Section

2.1. Sample Synthesis. Four samples were studied in this work with the following compositions of gels: $[\text{a}] = [\text{b}] = 0.4$ and $[\text{c}] = 1, 1.5, 2$ and 3. According to the earlier study of these materials,⁴ some of the F^- anions are replaced by the OH^- groups. The concentration of F^- anions x varies with pH, which in turn depends on the concentration of DEA. The unit cell formulas, $\text{Al}_{32}\text{P}_{32}\text{O}_{128}\text{TMAF}_x\text{TMAOH}_{8-x}$, as determined by the chemical analysis,⁴ are given in Table 1. Also shown in the table are the initial and final values of pH measured during the synthesis. The samples were studied in a dried, as-synthesized state.

2.2. NMR. The NMR experiments included ^1H MAS, ^{27}Al 3QMAS,⁶ $^{19}\text{F} \rightarrow ^{27}\text{Al}$ and $^1\text{H} \rightarrow ^{27}\text{Al}$ 3Q-REDOR⁷ and $^{19}\text{F} \rightarrow ^{27}\text{Al}$ dipolar decoupling (DD) 3QMAS.⁸ The ^1H MAS spectra were recorded on a Bruker ASX400 spectrometer using a 2.5-mm MAS probe and a sample rotation rate of 30 kHz. The 3QMAS spectra were collected at 7.1 and 9.4 T on Varian/Chemagnetics Infinity 300 and 400 spectrometers, both equipped with doubly tuned 3.2-mm MAS probes. These experiments used the z-filter MQMAS scheme⁹ with the RF fields of ~ 300 kHz and 17 kHz during the nonselective and selective pulses, respectively. The t_1 step of data acquisition was synchronized with the spinning rate of the rotor (20 kHz).¹⁰ The same RF conditions for ^{27}Al were used during DD-3QMAS and 3Q-REDOR experiments. The high-frequency channel used an RF field of 150 kHz for ^1H and ^{19}F . ^1H and ^{19}F decoupling was not used during the acquisition of ^{27}Al signal because it did not affect the resolution. The ^1H and ^{27}Al spectra reported in this work use the δ scale, with positive values downfield, and are referenced to tetramethylsilane (TMS) and aluminum nitrate aqueous solution.

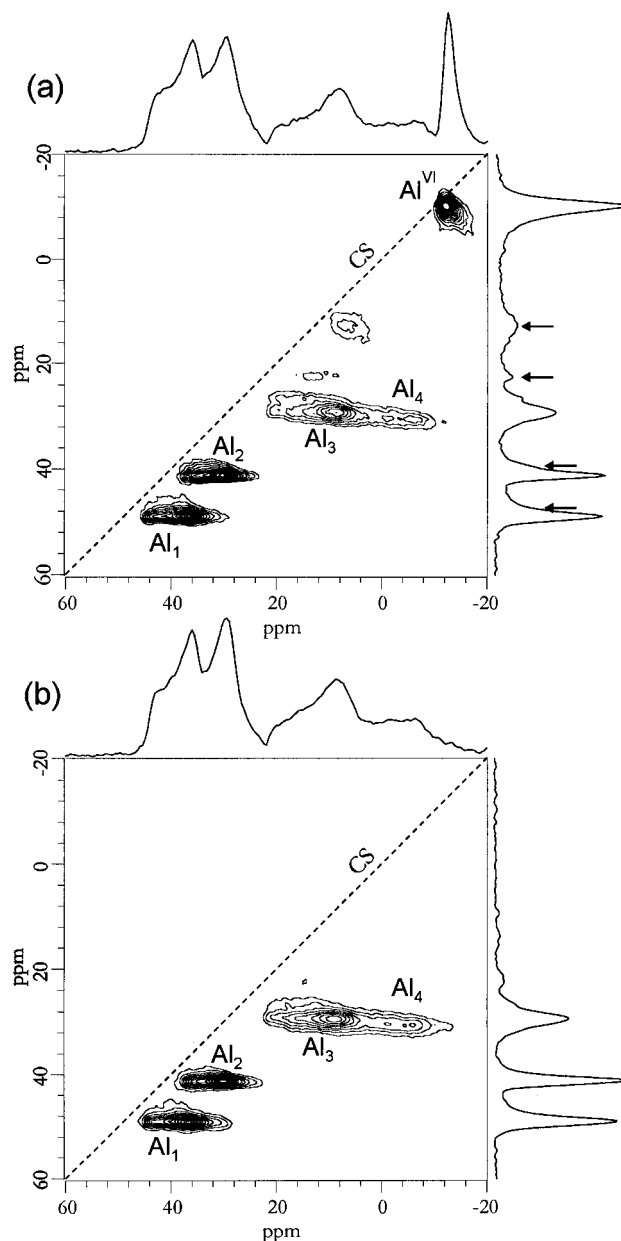


Figure 2. ^{27}Al 3QMAS sheared spectra of UiO-7 taken at 9.4 T: (a) sample 1, and (b) sample 2. Dashed lines correspond to the chemical shift axis.¹¹

3. Results and Discussion

3.1. Structural Purity of the Samples. From the results of XRD analysis, two four-coordinated (Al_1 , Al_2) and two pentavalent (Al_3 , Al_4) aluminum sites are expected in the structurally pure framework of UiO-7. Figure 2 shows two examples of ^{27}Al 3QMAS spectra of the studied samples. Sample 1, which was synthesized at a starting pH of 3.5, yielded the spectrum shown in Figure 2a. Since the 3QMAS spectra of samples 2, 3, and 4 are almost identical, only sample 2 is represented in Figure 2b. The resonances Al_1 through Al_4 are assigned to the corresponding sites in the structure of UiO-7 shown in Figure 1. These assignments are made on the basis of the distance measurements via MQ-REDOR, as described in Section 3.2. The isotropic chemical shift δ_{CS} and the quadrupole coupling C_Q can be easily obtained from MQMAS spectra (see Table 2).¹¹ It is noted that the intensities associated with these resonances are not in the ratio 1:1:1:1. This effect is common in MQMAS NMR, as the nuclei with different values of C_Q do

TABLE 2: Isotropic Chemical Shifts (δ_{CS}), Second-Order Quadrupolar Effect Parameter (P_Q), Aluminum–Fluorine and Aluminum–Hydrogen Distances Measured in This Work by NMR, and Aluminum–Fluorine Distances Determined in Ref 2 by XRD

species	δ_{CS} [ppm]	P_Q^a [MHz]	Al–F distances [Å]			Al–H distances [Å] ^d
			NMR ^b	NMR ^c	XRD	
Al ₁	50.6 ± 0.5	3.8 ± 0.2	3.7 ± 0.1	3.7 ± 0.1	3.69	3.0 ± 0.1
Al ₂	43.0 ± 0.5	3.6 ± 0.2	3.4 ± 0.1	3.3 ± 0.1	3.16	2.9 ± 0.1
Al ₃	27.2 ± 0.7	4.9 ± 0.3	2.1 ± 0.1	2.0 ± 0.1	1.90	2.85 ± 0.05
Al ₄	24 ± 1	6.3 ± 0.5	2.1 ± 0.1	2.0 ± 0.1	2.06	2.85 ± 0.05

^a $P_Q = C_Q \sqrt{1 + \frac{1}{3}\eta_Q^2}$. ^b Measured for sample 1. ^c Sample 3. ^d Sample 4.

not respond to excitation and conversion in the same manner.¹² Species Al₄, which experiences the strongest quadrupole interaction, is suppressed and is shifted the most from the so-called chemical shift axis in the MQMAS spectrum.¹¹ For species Al₃ and Al₄, the combination of chemical and quadrupolar induced shifts is such that their isotropic resonances strongly overlap at 9.4 T. However, we were able to separate these resonances in the 3QMAS spectrum obtained for sample 2 at 7.05 T. The MAS projection of this spectrum (not shown) is consistent with the ²⁷Al MAS spectrum measured in the original report on UiO-7.²

The 3QMAS spectrum of sample 1 shows additional ²⁷Al resonances, marked with arrows in Figure 2a, which cannot be assigned to the UiO-7 structure. We observed similar signals in this sample using the highly sensitive CPMG-3QMAS experiment¹³ (not shown). It is likely that these resonances are due to five- and four-coordinated Al sites in AlPO₄-AFR. The AlPO₄-AFR structure is known to consist of similar columns of [4⁴6²] units³ and its 3QMAS spectrum¹⁴ shows four ²⁷Al resonances close to those observed as a minor phase in sample 1. It is also noted that the ¹⁹F MAS spectrum of AlPO₄-AFR sample synthesized in the presence of HF exhibited the same resonance at −109 ppm¹⁵ as did UiO-7. Finally, the narrow line at −11 ppm, which is most intense in sample 1, corresponds to hexacoordinated aluminum atoms with a small value of C_Q . This resonance has been earlier observed in calcined UiO-7.² The ¹⁹F → ²⁷Al and ¹H → ²⁷Al 3Q-REDOR experiments (to be discussed later), show that the Al^{VI} species is at least 10 Å from the nearest fluorine. Thus, it is located outside of the lattice shown in Figure 1.

The above results show that the synthesis of UiO-7 is best performed when the starting pH is greater than 3.5. Most of the studies that follow used sample 3, which contained less than 5% of AFR impurities and no detectable amount of Al^{VI}.

3.2. Local Order. Figure 3 shows the result of a DD-3QMAS experiment between ¹⁹F and ²⁷Al in sample 3. In this experiment, the dipolar coupling between ¹⁹F and ²⁷Al spins is reintroduced by applying a series of rotor synchronized π pulses at the ¹⁹F frequency.⁸ This recoupling effect is best achieved when the π pulses are inserted during the triple quantum evolution. In such case a severe broadening of ²⁷Al resonances is observed along the isotropic projection, even in the presence of weak ¹⁹F–²⁷Al coupling.¹⁶ By comparing the isotropic projection of a standard 3QMAS spectrum (Figure 3a) with the corresponding DD-3QMAS spectrum (Figure 3b), it is evident that the F atoms are located closer to sites Al₃ and Al₄ than Al₁ and Al₂. Indeed, the F–Al₃ and F–Al₄ dipolar coupling is so large that these two resonances nearly disappear in the background noise of the DD-3QMAS spectrum.

To measure the ²⁷Al–¹⁹F and ²⁷Al–¹H distances, we performed the 3Q-t₂-REDOR experiments. The MQ-REDOR

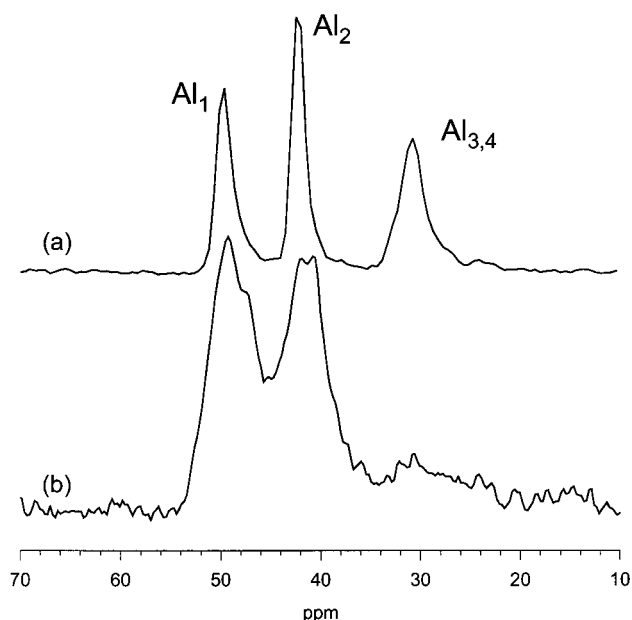


Figure 3. Isotropic projections of ²⁷Al 3QMAS spectra of sample 3: (a) standard 3QMAS spectrum, (b) DD-3QMAS spectrum obtained by introducing two π pulses per rotor period during t_1 .

method, described in detail elsewhere,⁷ employs two strong and two selective π pulses at the ²⁷Al frequency with phases cycled to select the coherence pathway $0 \rightarrow \pm 3 \rightarrow 0 \rightarrow +1 \rightarrow -1$. The second selective pulse creates two windows in which rotor-synchronized π pulses are applied at the ¹⁹F (or ¹H) frequency to restore the dipolar coupling. The results of MQ-REDOR experiment are best shown in form of the so-called REDOR difference curve,¹⁷ $\Delta S/S_0 = 1 - S(DN_c T_R)/S_0(DN_c T_R)$. This curve represents the normalized difference between spectra obtained without (S_0) and with (S) the dipolar dephasing pulses, versus the number N_c of rotor periods T_R during which they are applied. It is important to note that the REDOR curves depend only on the dipolar coupling D between the “targeted” spins. Other heterogeneous dipolar interactions, chemical shift anisotropy, J coupling, and the irreversible T_2 effects cancel in $\Delta S/S_0$. As has been shown earlier,¹⁶ the quadrupole interactions have negligible effect on $\Delta S/S_0$ because of the very strong RF field (300 kHz) used in the MQMAS experiment. Consequently, the analysis of the REDOR curves can be done using the standard formulas corresponding to an isolated pair of spin-1/2 nuclei.

The ¹⁹F → ²⁷Al 3Q-t₂-REDOR curves for Al₁ through Al₄ in sample 3 are shown in Figure 4. Continuous lines represent the best fits, while the dashed curves are calculated for distances modified by ±0.1 Å. The following internuclear distances are obtained: Al₁–F = 3.7 (±0.1) Å, Al₂–F = 3.3 (±0.1) Å, Al₃–F = 2.0 (±0.1) Å, and Al₄–F = 2.0 (±0.1) Å (see Table 2). The same results were obtained for sample 1. The distances between Al and F(OH) site in the [4⁴6²] subunit measured earlier by the XRD method are as follows: Al₁–F = 3.69 Å, Al₂–F = 3.16 Å, Al₃–F = 1.9 Å, and Al₄–F = 2.06 Å.² Thus, the NMR results show that the (only) fluorine species observed at −109 ppm in ¹⁹F MAS is indeed located inside the [4⁴6²] cage. Furthermore, based on the MQ-REDOR data, it is now possible to assign the Al resonances to the structural sites shown in Figure 1. Finally, no REDOR effect has been observed between F and Al^{VI}. This implies that the F–Al^{VI} distance is greater than 10 Å (we estimated that a fluorine atom at a lesser distance would have been detected under the conditions of our experiment).

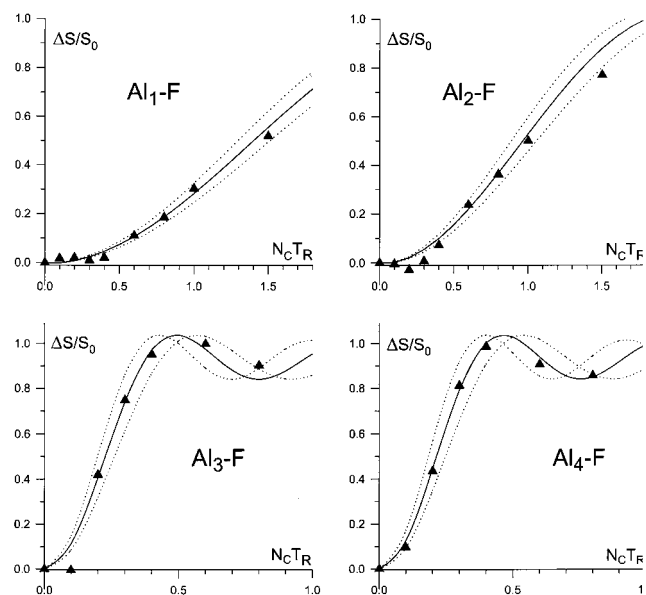


Figure 4. $^{19}\text{F} \rightarrow ^{27}\text{Al}$ 3Q- t_2 -REDOR curves corresponding to the four aluminum species in UiO-7 in sample 3.

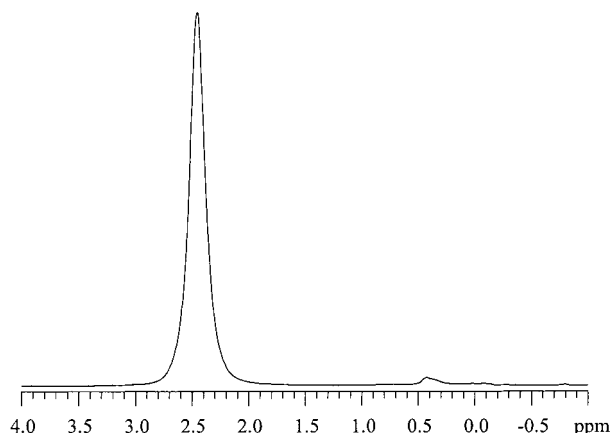


Figure 5. ^1H spectrum of sample 3 taken at 9.4 T under 30 kHz MAS.

In a similar way, the $^1\text{H} \rightarrow ^{27}\text{Al}$ 3Q- t_2 -REDOR curves were recorded for samples 1 and 4. All resulting internuclear distances are between 2.8 and 3.0 (± 0.2) Å. It is noted that the concentrations of OH groups in samples 1 and 4 differ by approximately 1 order of magnitude (see Table 1). Since the intensity of REDOR difference spectra was comparable in both samples, it appears that the OH groups did not play a significant role in these experiments. This result can be explained by noting that the TMA^+ template, which contains the methyl groups, is located in the center of $[4^6 6^4 8^4]$ cages. It is known that the three ^1H nuclei in a rotating methyl group produce a dipolar field equivalent to that of a single motionless proton located in their center of gravity.¹⁸ Since the diameter of $[4^6 6^4 8^4]$ cages is equal to 8 Å, it is evident that these groups are responsible for the observed ^1H – ^{27}Al distances. The OH protons in UiO-7 are expected to occupy a location that is approximately 1 Å above that of an F atom inside the $[4^4 6^2]$ subunits. In such case the ^1H – ^{27}Al distances should be ~ 2.5 Å for sites Al_3 and Al_4 , 19, 20, and ~ 3 Å for sites Al_1 and Al_2 . Thus, the presence of OH groups would have no notable effect on the outcome of our ^1H – ^{27}Al MQ-REDOR experiment in sample 4.

To obtain conclusive evidence of the presence of the OH groups, ^1H NMR spectra of all samples were acquired under MAS at 30 kHz. The resulting spectra are well resolved with an intense peak at 2.8 ppm assigned to hydrogen in TMA²¹ and

a weak resonance at 0.5 ppm that is consistent with the terminal AIOH group (see Figure 5).²⁰ Since the amount of TMA in the structure is well-known, the relative intensities between the two ^1H lines provide an accurate measure of the OH concentration in UiO-7. As is shown in Table 1, the NMR results are in relatively good agreement with the elemental analysis, which confirms that sample 1 has the highest concentration of F^- anions. We note that the complementary measurements of ^{19}F MAS spectra were also performed. However, the results were less accurate due to the long T_1 relaxation and the high fluorine background in our MAS probe.

4. Conclusion

The results of this work demonstrate that modern solid state NMR can reveal the structural details of powdered AlPO_4 -ZON materials and identify the impurities introduced during the synthesis. The UiO-7 sample obtained with $[c] = 2$ contained the least amount of structural impurities (Al^{VI} and/or AlPO_4 -AFR), but had a substantial amount of OH^- groups. On the other hand, the undesired phases were present in the sample with highest concentration of F^- . The $^{19}\text{F} \rightarrow ^{27}\text{Al}$ 3Q- t_2 -REDOR experiment provided accurate Al–F distances and allowed us to assign the ^{27}Al MQMAS spectra. The same methodology can now be applied in the studies of the effect of other synthesis parameters on the formation of these materials.

Acknowledgment. The authors thank Drs. J. L. Guth and L. Delmotte from the University of Mulhouse for providing the UiO-7 samples and Dr. D. Freude from the University of Leipzig for valuable discussions. This research was supported at Ames Laboratory by the U.S. Department of Energy, Office of Basic Energy Sciences, Division of Chemical Sciences, under Contract W-7405-Eng-82 and at the University of Lille by the CNRS and the Nord-Pas de Calais Region.

References and Notes

- Guth, J. L.; Kessler, H.; Caullet, P.; Hazm, J.; Merrouche, A.; Patarin, J. *Proc. 9th Intl. Zeolite Conf.* **1993**, *1*, 215.
- Akporiaye, D. E.; Fjellvag, H.; Halvorsen, E. N.; Hustveit, J.; Karlsson, A.; Lillerud, K. P. *J. Phys. Chem.* **1996**, *100*, 16641.
- Meier, W. M.; Olson, D. H.; Baerlocher, C. *Atlas of Zeolite Structure Types*, 4th ed.; Elsevier: New York, 1996.
- Sierra, L.; Patarin, J.; Guth, J. L. *Microporous Mater.* **2000**, *38*, 123.
- Wilson, S. T.; Lok, B. M.; Messina, C. A.; Cannan, T. R.; Flanigen, E. M. *J. Am. Chem. Soc.* **1982**, *104*, 1146.
- Frydman, L.; Harwood, J. S. *J. Am. Chem. Soc.* **1995**, *117*, 5367.
- Fernandez, C.; Lang, D. P.; Amoureux, J. P.; Pruski, M. *J. Am. Chem. Soc.* **1998**, *120*, 2672.
- Pruski, M.; Fernandez, C.; Lang, D. P.; Amoureux, J. P. *Catal. Today*, **1999**, *49*, 401.
- Amoureux, J. P.; Fernandez, C.; Steuernagel, S. *J. Magn. Reson.* **1996**, *A123*, 116.
- Massiot, D. *J. Magn. Reson.* **1996**, *A122*, 240.
- Amoureux, J. P.; Fernandez, C. *Solid State NMR* **1998**, *10*, 221.
- Amoureux, J. P.; Fernandez, C.; Frydman, L. *Chem. Phys. Lett.* **1996**, *259*, 347.
- Vosegaard, T.; Larsen, F. H.; Jakobsen, H. J.; Ellis, P. D.; Nielsen, N. C. *J. Am. Chem. Soc.* **1997**, *119*, 9055.
- Delmotte, L. Private communication.
- Estermann, M. A.; McCusker, L. B.; Baerlocher, C. *J. Appl. Crystallogr.* **1992**, *25*, 539.
- Pruski, M.; Bailly, A.; Lang, D. P.; Amoureux, J. P.; Fernandez, C. *Chem. Phys. Lett.* **1999**, *307*, 35.
- Gullion, T.; Schaefer, J. *J. Magn. Reson.* **1989**, *81*, 196.
- Goetz, J. M.; Schaefer, J. *J. Magn. Reson.* **1997**, *127*, 147.
- Hunger, M.; Freude, D.; Fenzke, D.; Pfeifer, H. *Chem. Phys. Lett.* **1991**, *191*, 391.
- Hunger, M. *Catal. Rev.-Sci. Eng.* **1997**, *39*, 345.
- Sasaki, S.-I. *Handbook of proton-NMR spectra and data*; Academic Press: Orlando, 1985.